2mix

X-922-74-98
PREPRINT

NASA TM X- 70628

A GLOBAL MAGNETIC ANOMALY MAP

(NASA-TM-X-70628) A GLOBAL MAGNETIC ANOMALY MAP (NASA) N74-20982
CSCL 08E
Unclas
G3/13 36513

R. D. REGAN
J. C. CAIN
W. M. DAVIS

APRIL 1974

GLOBAL GEOMAGNETISM PROJECT

GODDARD SPACE FLIGHT CENTER
Greenbelt, Maryland

U. S. GEOLOGICAL SURVEY
Reston, Virginia

For information concerning availability
of this document contact:

Technical Information Division, Code 250
Goddard Space Flight Center
Greenbelt, Maryland 20771

(Telephone 301-982-4488)

X-922-74-98
PREPRINT

A GLOBAL MAGNETIC ANOMALY MAP

R. D. Regan and W. M. Davis
U. S. Geological Survey
Silver Spring, Maryland 20910

and

J. C. Cain
NASA/Goddard Space Flight Center
Greenbelt, Maryland 20771

April 1974

GODDARD SPACE FLIGHT CENTER
Greenbelt, Maryland

/

A GLOBAL MAGNETIC ANOMALY MAP

R. D. Regan*, J. C. Cain**, and W. M. Davis*

ABSTRACT

A subset of POGO satellite magnetometer data has been formed that is suitable for analysis of crustal magnetic anomalies. Using a thirteenth order field model, fit to these data, magnetic residuals have been calculated over the world to latitude limits of ±50°. These residuals averaged over one degree latitude-longitude blocks represent a detailed global magnetic anomaly map derived solely from satellite data. Preliminary analysis of the map indicates that the anomalies are real and of geological origin.

Preceding page blank

*U.S. Geological Survey, Silver Spring, Md. 20910
**NASA/Goddard Space Flight Center, Greenbelt, Md. 20771

TABLE OF CONTENTS

Preceding page blank

A GLOBAL MAGNETIC ANOMALY MAP

INTRODUCTION

The U. S. Geological Survey and Goddard Space Flight Center (NASA) are jointly involved in an analysis of presently available magnetic data from the Cosmos-49 (Benkova et al., 1971) and OGO-2, 4, and 6 (POGO) (Cain and Langel, 1971) satellites. The major objective of this analysis is the identification of anomalies having geological significance.

Previous reports have established the gross correlation between aeromagnetic surveys and satellite measurements over broad areas and that magnetic anomalies associated with inhomogenieties in the lithosphere should be detectable at satellite altitudes (Zietz et al., 1970; Andreasen et al., 1970). The first confirmation of the existence of such an anomaly in the satellite data was the identification of the Bangui anomaly (Regan et al., 1973a). This anomaly, occuring over central Africa, was discovered in a detailed analysis of the POGO data and later identified on Project MAGNET (Stockard, 1971) data.

The data reduction procedures employed to define the Bangui anomaly have now been applied to the entire set of POGO magnetic measurements. It was thus possible to produce a detailed global magnetic anomaly map. The resolution of this map permits the identification of anomalies with wavelengths less than 14°. This represents a substantial increase in resolution over previous analyses (Benkova et al., 1973; Regan et al., 1973b). The anomalies noted on these earlier maps termed "intermediate size" anomalies, were of half wavelengths of approximately 19° and not clearly of lithospheric origin.

DATA SELECTION AND ANOMALY CALCULATION

At satellite altitudes, the anomaly signal is comparable in magnitude to time variations from external sources, therefore the satellite data must be obtained when the field is undisturbed. Also, the rapid decay of the signal with altitude requires that measurements be obtained at as low an altitude as possible. To obtain such data, the POGO observations, made during a period of variable magnetic activity and over an altitude range of 400 to 1500 km, had to be screened for low altitude and minimal magnetic activity.

A subset of the POGO data was constructed by screening the observations on altitude, local time, and Planetary Magnetic Activity Index (Kp) (Sugiura and Heppner, 1968, p. 72). Only data collected when Kp was less than, or equal to

2^+ were utilized. These data were corrected for disturbance effects by the method described by Davis and Cain (1973). Because of the limitations of this disturbance correction, the data were further restricted to geographic latitudes less than, or equal to $\pm 50^\circ$. Of this set, data collected at altitudes greater than 700 km and at local times between 0900 and 1500 were rejected. The local time selection was made to avoid magnetic effects due to the equatorial electrojet and ionospheric currents (Cain and Sweeney, 1973). This screening of the data provided a subset of 393,452 observations with a 7 second or 50 km spacing along a given orbit and good geographic distribution (typically 15 observations per 1° latitude-longitude block).

The method utilized to determine an anomaly is a regional-residual field separation where the regional field is defined by a four-dimensional (latitude, longitude, altitude, time) function (Cain et al., 1967). This function is computed by least squares fitting of a spherical harmonic series to the observed data. The series is truncated at a harmonic order where the root mean square of the fit does not decrease significantly by computing higher order coefficients or at some prior arbitrary point necessitated by computer capacity. The anomalies or residuals, termed ΔF, are defined as the difference between the measured and computed values at each observation.

The validity of field residuals at satellite altitudes has been determined by comparing residual values derived from two completely independent sets of observations and field references (Regan et al., 1973b).

WORLD MAP

A thirteenth order spherical harmonic series (or field model) was fit to the subset of POGO data. Magnetic field residuals were calculated and averaged over one degree latitude-longitude blocks. The resulting global magnetic anomaly map, contoured at 2 gammas, exhibited some north-south striping that was a reflection of the direction of the POGO orbits. A preliminary attempt to reduce some of the noise in the map was accomplished by deleting the ± 2 gamma contours that were not associated with more intense anomalies; that is, only anomalies with absolute magnitude greater than 2 gammas were retained. This filtered map is shown in Figure 1. This map represents one degree averaged magnetic residuals at a mean elevation of 520 km. The residuals are not at a common elevation, but on a topographic surface defined by the averaged elevations of the data in each one degree block. However, the anomalies are not considered to be significantly distorted by this variation in altitude. Only minor changes in anomaly structure were noted in the reduction to a common plane of a 20 by 20 degree area of this map over the Bangui anomaly (Regan et al., 1973a).

The maximum and minimum anomaly values are +10 and -12 gammas respectively. Colors were utilized to simplify the complex structure of the map. Color changes occur at the contour interval of two gammas. The red end of the spectrum is associated with positive anomalies and the blue end with negative anomalies. Specifically, the colors used in this figure are: purple, -4 gammas and below; dark blue, -4 to -2 gammas; light blue, -2 to 0 gammas; green, 0 to +2 gammas; yellow, 2 to 4 gammas, orange, 4 to 6 gammas; pink, 6 to 8 gammas, and red, 8 gammas and above.

Several features are immediately apparent in the global magnetic anomaly map (Fig. 1). Most striking is the apparent lack of anomalies in the Pacific Ocean with the exception of a pair of anomalies (+6 gammas and -6 gammas amplitude) in the area where the Emperor Seamount chain and the Hawaiian Island chain intersect. Also evident is the Bangui anomaly, a 12 gamma low, over central Africa.

The Bangui anomaly is a confirmed magnetic anomaly of possible lithospheric origin. Because of this it is presumed that the other magnetic anomalies shown are also real and of internal origin. However, it is possible that a few of the anomalies could be artifacts of spurious orbits, insufficient time corrections, and other data reduction procedures. Thus, the validity of all the anomalies is now being investigated by several approaches.

First the anomaly structure as revealed on individual satellite passes is being examined. The anomalies shown on individual passes are not affected by the averaging technique used to construct the map. Also, persistence of an anomaly in satellite observations made at various local times and at various elevations would indicate that the anomaly was real and not the result of any external field effects. The magnetic field residuals on several POGO satellite passes over India are shown in Figure 2. The magnetic high over the southern part of India and the low over the Himalaya Mountains are shown to persist on all satellite passes. The anomalies are independent of local time and show a dependence on altitude that is consistent with an internal origin.

Another method of investigating the validity of these anomalies is by comparing them to Project MAGNET (aeromagnetic) data. The available Project MAGNET data over several anomalous areas of the satellite map have been examined and in each case there is evidence of an anomaly. The signals associated with the Bangui magnetic anomaly have been compared by continuing the Project MAGNET data to satellite altitude, as shown in Figure 3. This represents a segment of Project MAGNET Line T217 over the Bangui magnetic anomaly. Assuming a two-dimensional source the profile was mathematically continued to satellite altitude and compared to a satellite profile. The comparison demonstrates that the same anomaly is being measured by both satellite and aircraft magnetometers. The magnitude of the anomaly at aircraft elevation (-780 gamma) compared to that at satellite elevation (-16 gammas) is also consistent with a magnetic anomaly of internal origin.

An alternative approach is to compare the POGO magnetic anomalies with a similar reduction of the Cosmos-49 data. Such a comparison at longer wavelengths was made by Regan et al., (1973b) and demonstrated a correlation between the two data sets. However, it was noted then that the Cosmos data are much less numerous than the POGO observations. Also, the limited orbital information in the Cosmos data is a source of error in the reduction of the magnetic measurements. Hence it was not thought that any meaningful results are avilable with a one degree averaging of the Cosmos data. Nevertheless a thirteenth order field model was fit to the Cosmos-49 data. As expected, the scatter in this fit was much higher (38 gammas rms) than that of the POGO model (7 gammas rms), and the data set was not dense enough for averaging over one degree latitude-longitude blocks. However, a map of the Cosmos residuals using this model averaged over five degree latitude-longitude blocks was constructed. Although the five degree averaged map is not as detailed as the POGO one degree averaged map (Fig. 1) the general location of the anomalies on both maps is consistent. An example is shown in Figure 4. This shows the Cosmos-49 data over the African continent. The POGO data, averaged on one degree latitude-longitude blocks, over the same area is shown in Figure 5. In general there is a good correlation between the two maps, particularly over the southern half of the continent. The distortions in the Cosmos map are primarily a result of the sparse nature and nonuniform distribution of the data. The number of Cosmos observations per five degree block in this area ranges from 1 to 23. Whereas the number of POGO observations ranges from 300 to 450 per five degree block. There is also a distortion of the anomalies along the flight path of the Cosmos satellite (inclination ~ 50 degrees), similar to the north-south striping seen on the POGO map (Fig. 1).

Origin of the Anomalies

It is suspected that the anomalies shown in this map are primarily of geologic origin with a source in the lithospheric region of the earth.

The occurrence of these anomalies on all satellite passes, independent of local time and their decay with altitude, imply a definite internal origin for the source of these anomalies. Due to the use of a thirteenth order field model, the anomaly half wavelengths are less than 14° ($\simeq 180^\circ/13$) (Kaula, 1967) and this short wavelength end of the geomagnetic spectrum has been attributed to the crustal component of the geomagnetic field (Alldredge et al., 1963). Also by considering the rate of decay of anomalies described by the fourteenth harmonic, an estimate of the magnetic intensity of the source relative to the satellite anomalies can be calculated. A source in the lower mantle or at the mantle-core boundary would require an amplitude several thousand times as intense, whereas a source in the upper mantle or crust would need to be only an order of magntiude more intense.

A second approach to the identification of the satellite magnetic anomalies as lithospheric is to examine their correlation with known tectonic, geologic, or geophysical dàta. This is now being done in detail for the African continent. An example is shown in Figure 5. Here a tectonic map of Africa (from Wyllie, 1971), is shown with the POGO satellite magnetic data. The color scheme for the tectonic map is the same as that shown in Figure 6. Note that the color scheme for the magnetic map differs slightly from that of Figure 1. In this map the contour interval is 2 gammas and purple represents -6 gammas and below; dark blue, -6 to -4 gammas; light blue, -4 to -2 gammas; green -2 to -0 gammas; yellow, 0 to +2 gammas; orange, 2 to 4 gammas; pink, 4 to 6 gammas; and red, 6 gammas and above.

In considering the magnetic anomalies in this figure and Figure 6, it must be noted that the inclination of the main field is varying as a function of latitude. Thus, anomalies, due to induction, having similar origins would have different magnetic signatures at various geomagnetic latitudes.

In the center of the magnetic anomaly map is the Bangui anomaly that occurs over the tectonic uplift zone between the Chad and Congo Basins. South of the Bangui anomaly there is a general correlation of magnetic highs with continental shield areas and magnetic lows with continental platforms. The low at the southern tip of the continent is coincident with the Karroo Basin. The correlation appears reversed on the other side of the magnetic equator. The major magnetic high in the northwest part of Africa is situated over the El-Juf or Taudine Basin and the magnetic low east of this occurs over the uplift area between this basin and the Chad Basin.

For the general correlation on a global scale the filtered map (Fig. 1) is shown overlain on a tectonic map of the world (from Wyllie, 1971) in Figure 6. Only the contour lines from the magnetic map are shown. Figure 1 will have to be examined to determine the sense of the anomalies. Some correlations between the tectonic and magnetic maps are obvious. The continental shields in the southern hemisphere, and India in the north, all have magnetic highs associated with them. There is a considerable amount of magnetic structure in the vicinity of oceanic ridges contrasted with the central Pacific region that is devoid of anomalies.

CONCLUSION

Analysis of the POGO satellite data has resulted in a detailed global magnetic anomaly map. Verification of several distinct anomalies was obtained by examining individual satellite profiles and Project MAGNET data. The persistence of the anomalies on all satellite passes, independent of local time, demonstrate that they are real and not the effect of any magnetospheric or ionospheric disturbance. The rate of decay of the anomalies with altitude as observed in the aircraft and satellite data imply an internal origin for these anomalies. The limited analysis of the Cosmos data reveals a similar global distribution of anomalies which are more intense. This is consistent with an internal origin because the Cosmos-49 satellite was at a lower mean elevation (~375 km) than the POGO satellites. Although much more work is needed to fully interpret the map and determine the causes of these anomalies, the initial comparisons with tectonic maps are quite encouraging.

These results further demonstrate the utility of a satellite magnetometer as a geological/geophysical tool. A proposed global survey at low altitude using a vector magnetometer would provide the increased resolution necessary for more detailed geological description.

REFERENCES

Alldredge, L. R., G. D. Van Voorhis and T. N. Davis, 1963, A Magnetic Profile Around the World, Jor. Geophys. Research, v. 68, no. 12, p. 3679.

Andreasen, G. E., J. C. Cain, W. M. Davis and I. Zietz, 1970, Comparative Study of Cosmos-49 and OGO Satellite Magnetometer Measurements, presented at 40th annual meeting, S. E. G.

Benkova, N. P. and Sh. Sh. Dolginov, 1971, The Survey with Cosmos-49, in World Magnetic Survey, 1957-1969; Internat. Assoc. Geomagnetism and Aeronomy, Bull. No. 28, p. 75-77.

Benkova, N. P., Sh. Sh. Dolginov and Simonenko, 1973, Residual Geomagnetic Field from the Satellite Cosmos-49, Jour. Geophys. Research, v. 78, no. 5, p. 798.

Cain, J. C., S. J. Hendricks, R. A. Langel and W. V. Hudson, 1967, A proposed model for the international geomagnetic reference field - 1965, Jour. of Geomag. and Geoelec., Vol. 19, no. 4, p. 335.

Cain, J. C. and R. A. Langel, 1971, Geomagnetic survey by the polar orbiting geophysical observatories, in World magnetic survey, Internat. Assoc. Geomagnetism and Aeronomy., Bull. No. 28, p. 65-74.

Cain, J. C. and R. E. Sweeney, 1973, The POGO data, Jour. of Atmos. and Terr. Physics, v. 35, p. 1231.

Davis, W. M. and J. C. Cain, 1973, Removal of DS from POGO satellite data (Abs.), EOS, Transactions of AGU v. 54, no. 4, p. 242.

Kaula, W. M., 1967, Theory of Statistical Analysis of Data Distributed Over a Sphere, Reviews of Geophysics, vol. 5, no. 1, p. 83.

Regan, R. D., W. M. Davis and J. C. Cain, 1973a, The Bangui Magnetic Anomaly (Abs.), EOS, transactions of AGU, v. 54, no. 4, p. 236.

Regan, R. D., W. M. Davis and J. C. Cain, 1973b, The detection of "Intermediate" size magnetic anomalies in Cosmos-49 and OGO 2, 4, 6 data, in Space Research vol. XIII, p. 619-623.

Stockard, H. P., 1971, Worldwide surveys by Project Magnet, in World Magnetic Survey, 1957-1969; Internat. Assoc. Geomagnetism and Aeronomy, Bull. No. 28, p. 60-64.

Sugiura, M., and J. P. Heppner, 1968, The Earth's Magnetic Field, in Introduction to Space Science, 2nd ed., edited by W. N. Hess and G. D. Mead, Gordon and Breach, New York.

Wyllie, P. J., 1971, The Dynamic Earth: Textbook in Geoscience, John Wylies and Sons, Inc., New York, p. 9.

Zietz, I., G. E. Andreasen and J. C. Cain, 1970, Magnetic anomalies from satellite magnetometer: Jour. Geophys. Research, vol. 75, No. 20, p. 4007.

Figure 1. Global Magnetic-Anomaly Map; Contour Intervals, 2 gammas.

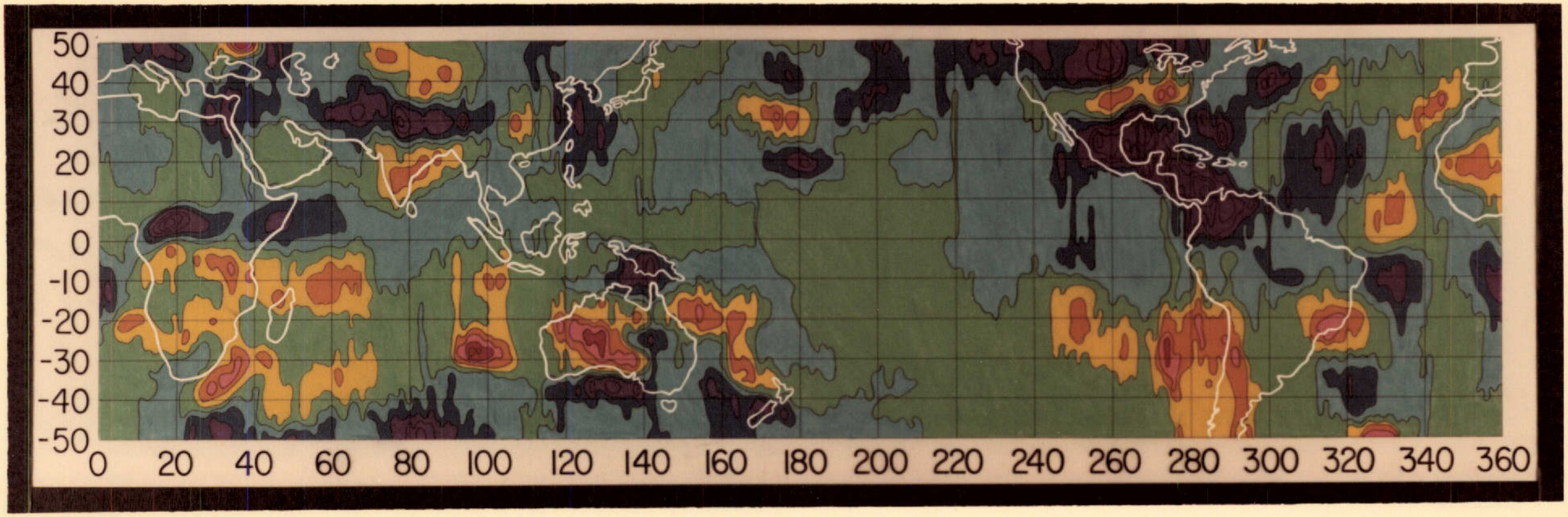
50
40
30
20
10
0
-10
-20
-30
-40
-50
0
20
40
60
80
100
120
140
160
180
200
220
240
260
280
300
320
340
360

Figure 2. Magnetic Field Residuals from Individual POGO Satellites. Passes over India; Note the magnetic high over Southern part of India and the low over Himalaya Mountains.

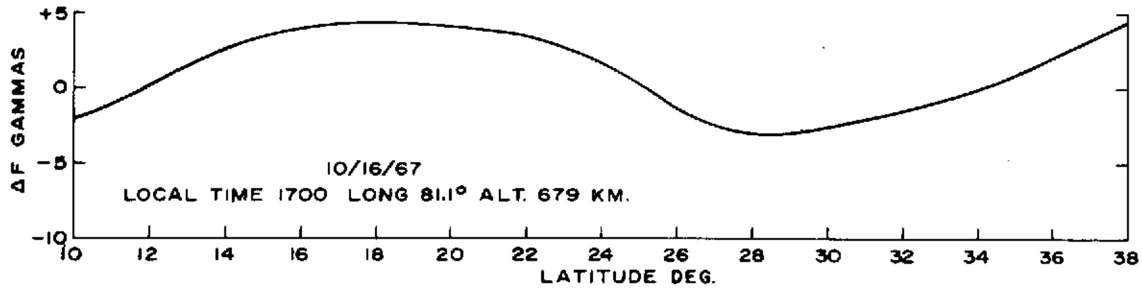
+5
0
-5
-10
ΔF GAMMAS
10/16/67
LOCAL TIME 1700 LONG 81.1° ALT. 679 KM.
10
12
14
16
18
20
22
24
26
28
30
32
34
36
38
LATITUDE DEG.

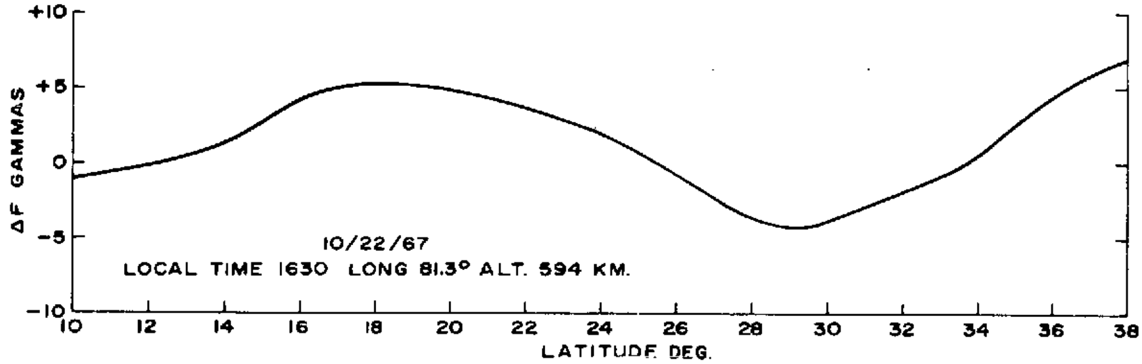
+10
+5
0
-5
-10
ΔF GAMMAS
10/22/67
LOCAL TIME 1630 LONG 81.3° ALT. 594 KM.
10
12
14
16
18
20
22
24
26
28
30
32
34
36
38
LATITUDE DEG.

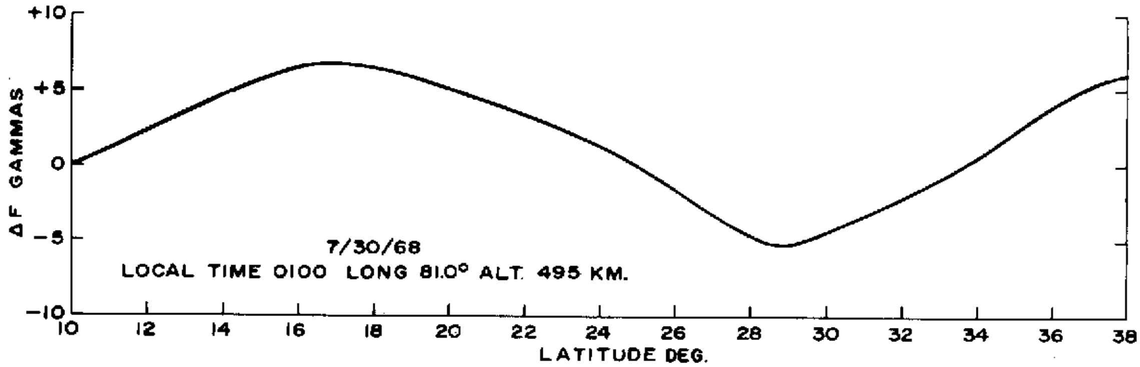
+10
+5
0
-5
-10
ΔF GAMMAS
7/30/68
LOCAL TIME 0100 LONG 81.0° ALT. 495 KM.
10
12
14
16
18
20
22
24
26
28
30
32
34
36
38
LATITUDE DEG.

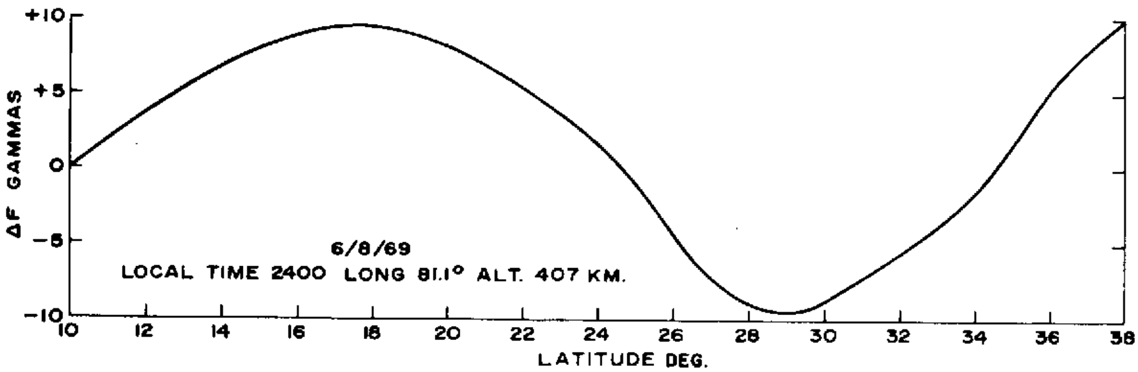
+10
+5
0
-5
-10
ΔF GAMMAS
6/8/69
LOCAL TIME 2400 LONG 81.1° ALT. 407 KM.
10
12
14
16
18
20
22
24
26
28
30
32
34
36
38
LATITUDE DEG.

Figure 3. A Comparison of Bangui Magnetic-Anomaly at OGO Satellite and Aircraft Altitudes.

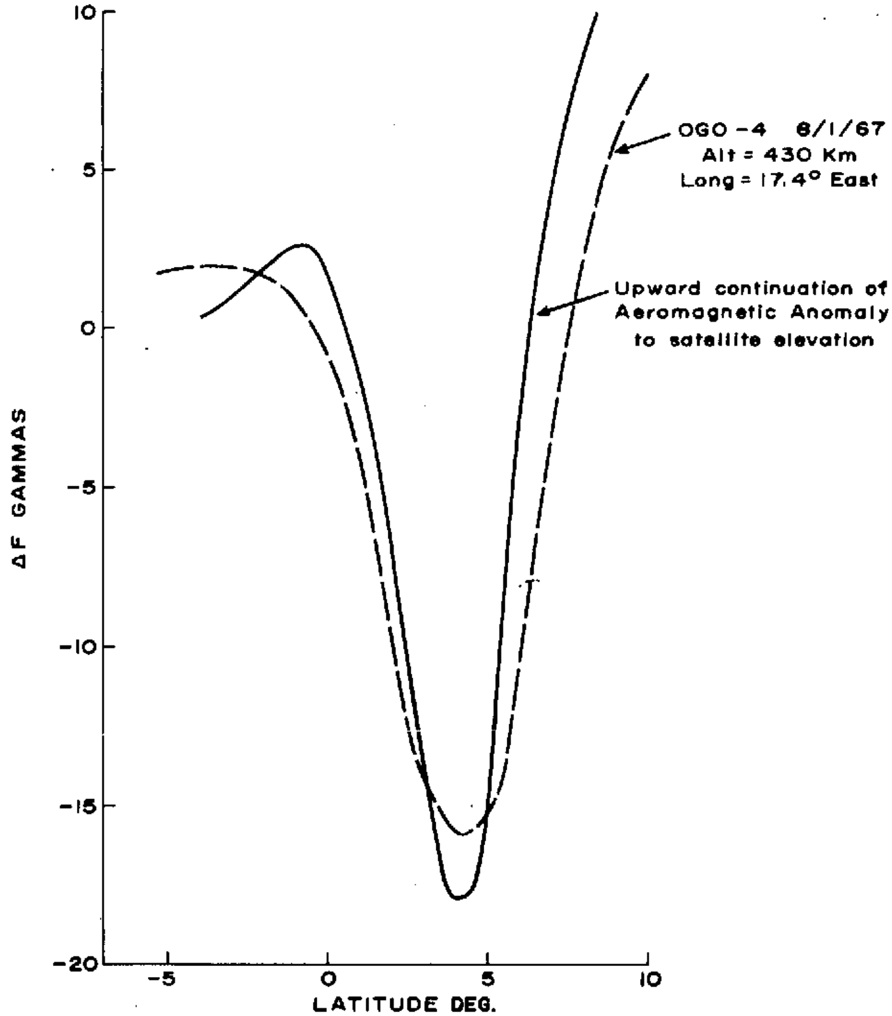
10
5
0
-5
-10
-15
-20
ΔF GAMMAS
-5
0
5
10
LATITUDE DEG.
OGO-4 8/1/67
Alt = 430 Km
Long = 17.4° East
Upward continuation of
Aeromagnetic Anomaly
to satellite elevation

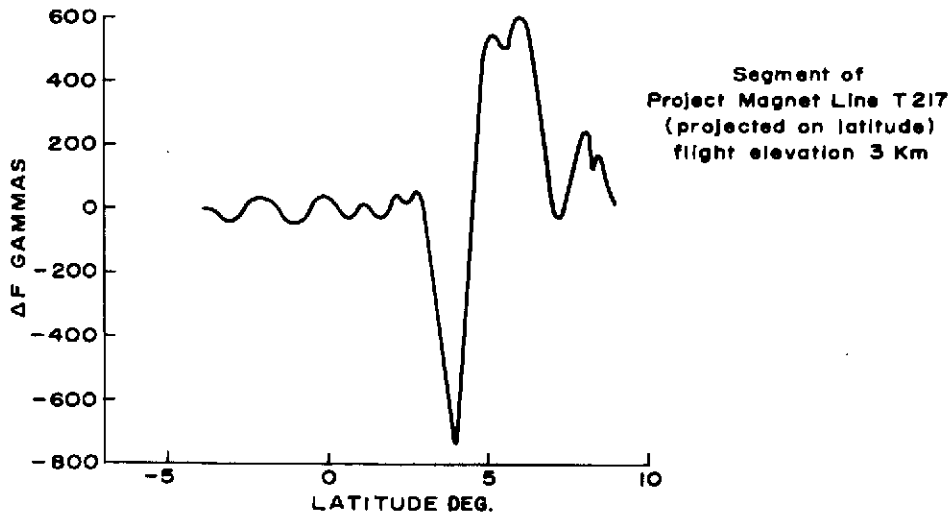
600
400
200
0
-200
-400
-600
-800
ΔF GAMMAS
-5
0
5
10
LATITUDE DEG.
Segment of
Project Magnet Line T217
(projected on latitude)
flight elevation 3 Km

Figure 4. Five Degree Averaged Cosmos-49 Magnetic Anomaly Map over Africa

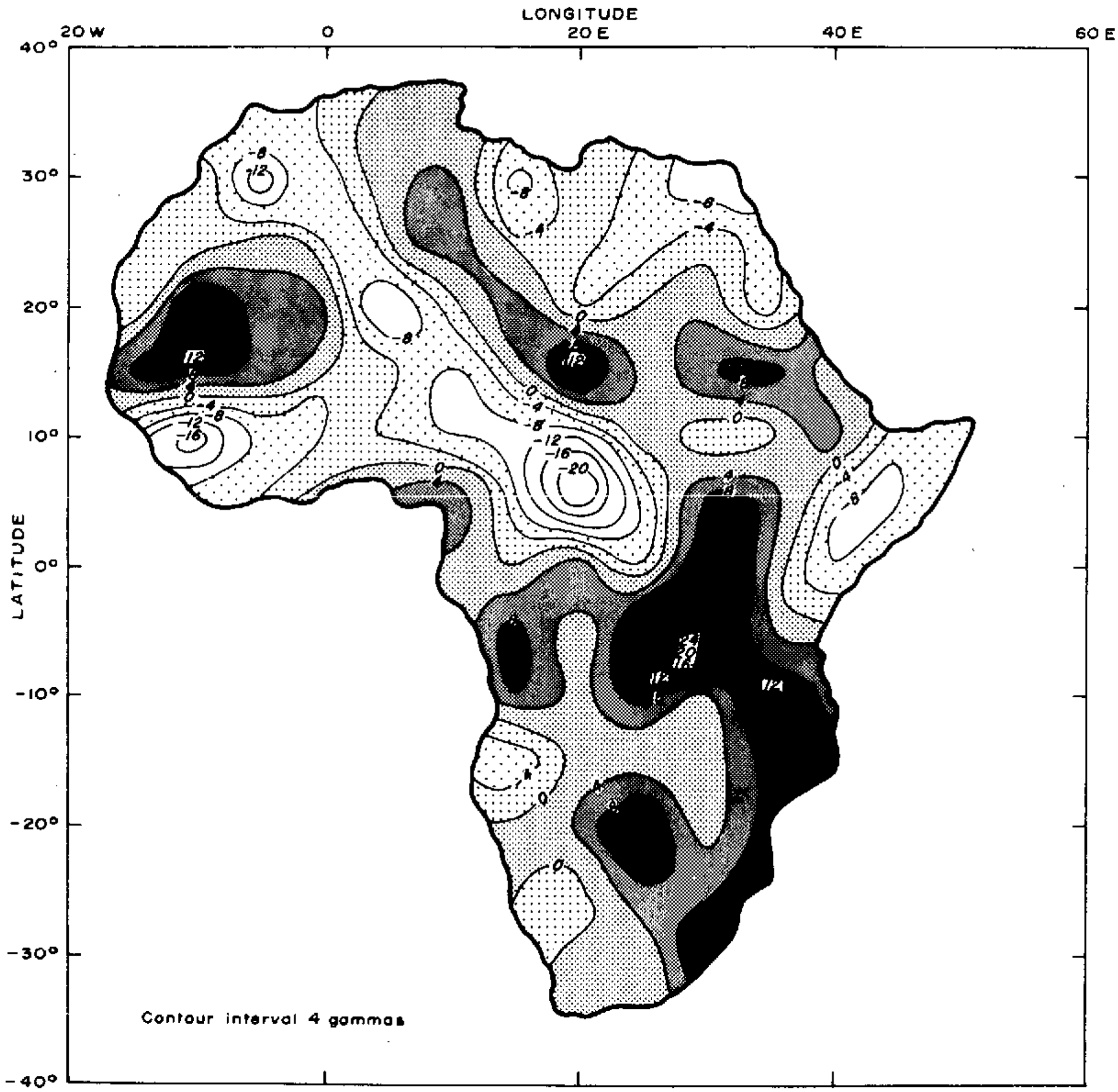
LONGITUDE
20 W
0
20 E
40 E
60 E
40°
30°
20°
10°
0°
-10°
-20°
-30°
-40°
LATITUDE
Contour interval 4 gammas

Figure 5. Tectonic and POGO Satellite Magnetic-Anomaly Maps Over Africa (tectonic map from Wyllie, 1971); Contour Intervals, 2 gammas.

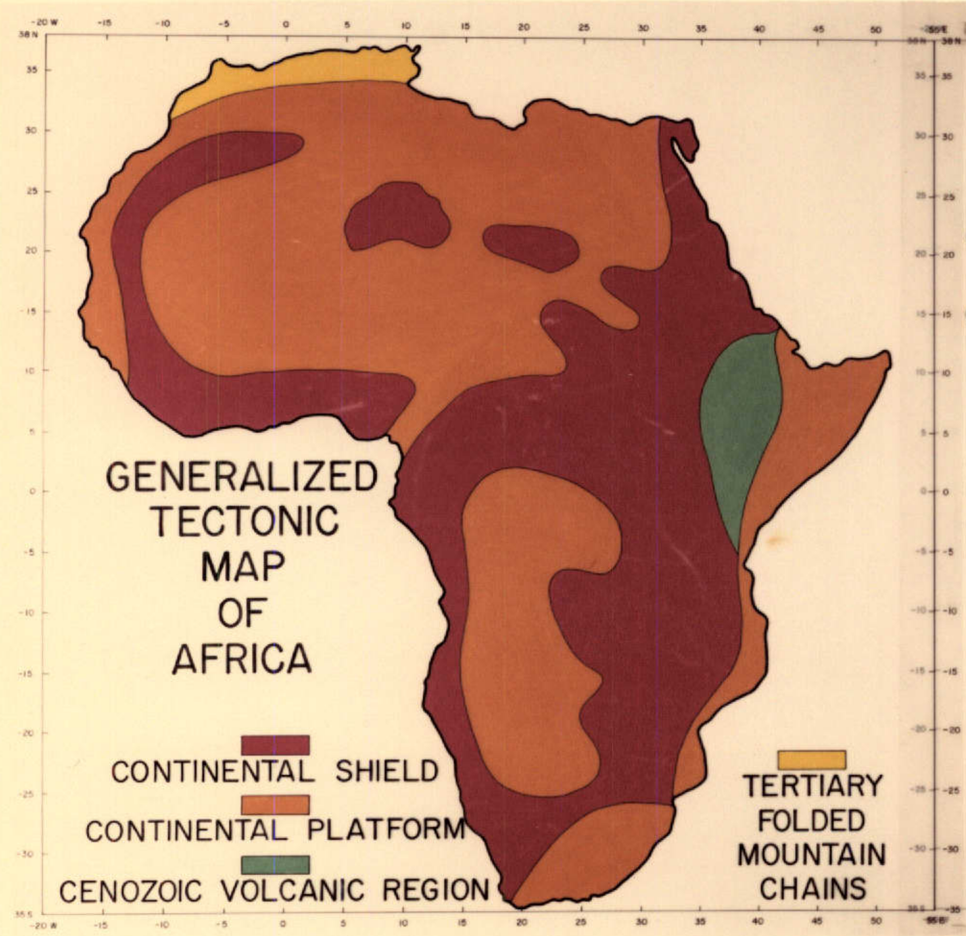
GENERALIZED
TECTONIC
MAP
OF
AFRICA
CONTINENTAL SHIELD
CONTINENTAL PLATFORM
CENOZOIC VOLCANIC REGION
TERTIARY
FOLDED
MOUNTAIN
CHAINS

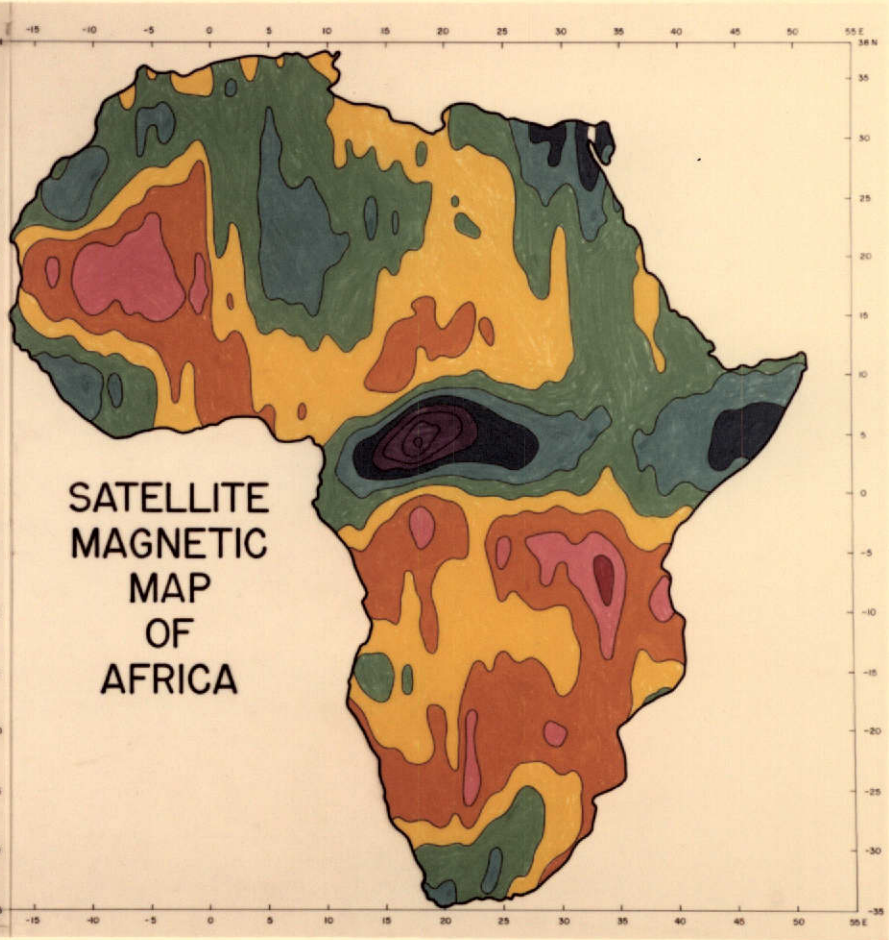
SATELLITE
MAGNETIC
MAP
OF
AFRICA

17

Figure 6. Global Tectonic Map Combined with the Contours of the Satellite Magnetic-Anomaly Map (tectonic map from Wyllie, 1971); Contour Intervals, 2 gammas.

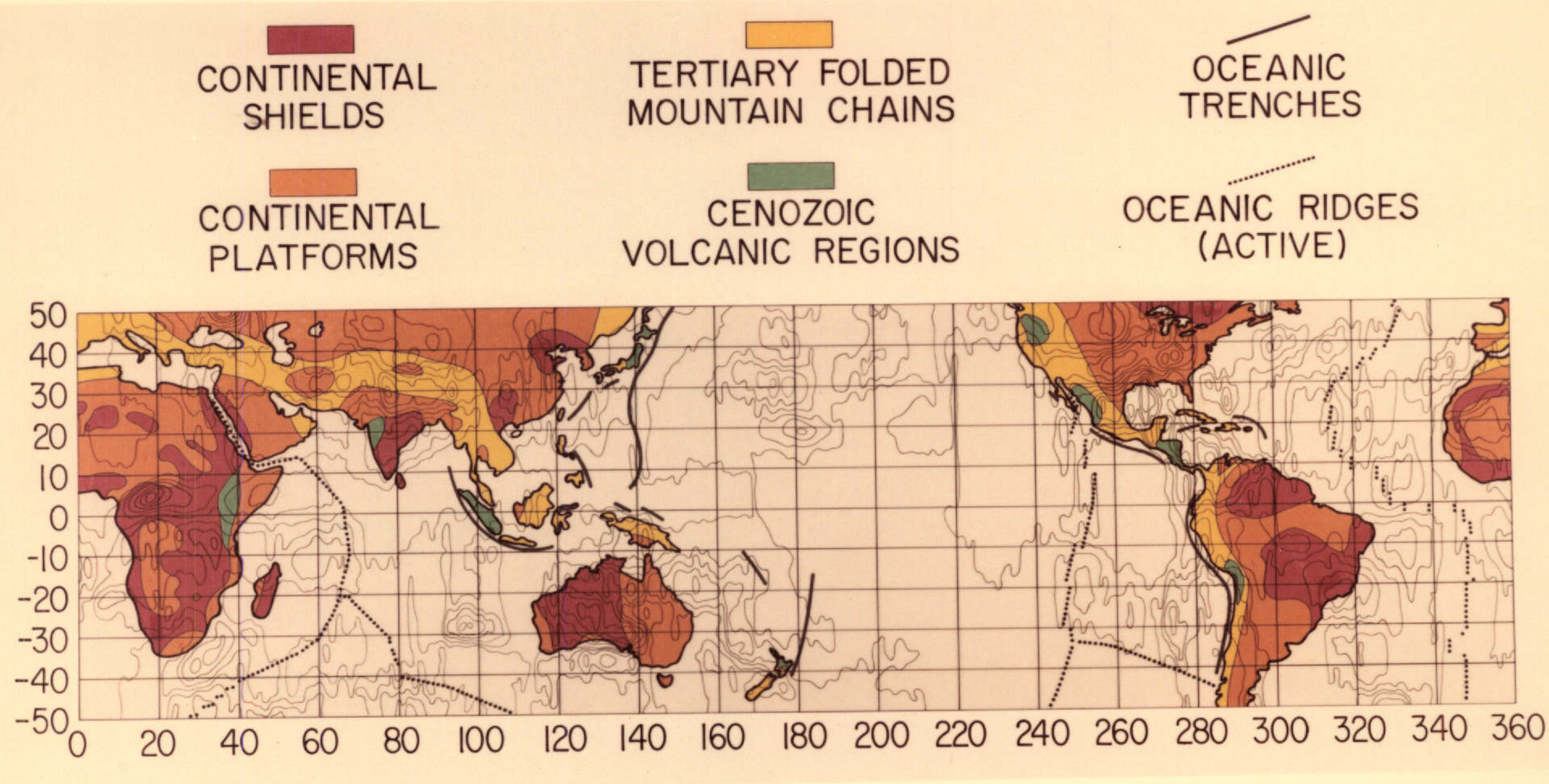
CONTINENTAL SHIELDS
TERTIARY FOLDED MOUNTAIN CHAINS
OCEANIC TRENCHES
CONTINENTAL PLATFORMS
CENOZOIC VOLCANIC REGIONS
OCEANIC RIDGES (ACTIVE)
50
40
30
20
10
0
-10
-20
-30
-40
-50
0
20
40
60
80
100
120
140
160
180
200
220
240
260
280
300
320
340
360

19